



Hydrogen Utilization Potential in Subsurface Sediments

Rishi R. Adhikari^{1,2*}, Clemens Glombitza³, Julia C. Nickel^{2,4}, Chloe H. Anderson⁵, Ann G. Dunlea⁵, Arthur J. Spivack⁶, Richard W. Murray⁵, Steven D'Hondt⁶ and Jens Kallmeyer^{2,4}

¹ MARUM - Center for Marine Environmental Sciences, University of Bremen, Bremen, Germany, ² Geomicrobiology Group, Institute of Earth and Environmental Science, University of Potsdam, Potsdam, Germany, ³ Center for Geomicrobiology, Department of Bioscience, Aarhus University, Aarhus C, Denmark, ⁴ Helmholtz-Centre Potsdam - GFZ German Research Centre for Geosciences, Potsdam, Germany, ⁵ Department of Earth and Environment, Boston University, Boston, MA, USA, ⁶ Graduate School of Oceanography, University of Rhode Island, Kingston, RI, USA

OPEN ACCESS

Edited by:

Jennifer Glass,
Georgia Institute of Technology, USA

Reviewed by:

John R. Spear,
Colorado School of Mines, USA
Eric Boyd,
Montana State University, USA

*Correspondence:

Rishi R. Adhikari
adhikari@uni-bremen.de

Specialty section:

This article was submitted to
Microbiological Chemistry and
Geomicrobiology,
a section of the journal
Frontiers in Microbiology

Received: 15 June 2015

Accepted: 06 January 2016

Published: 26 January 2016

Citation:

Adhikari RR, Glombitza C, Nickel JC, Anderson CH, Dunlea AG, Spivack AJ, Murray RW, D'Hondt S and Kallmeyer J (2016) Hydrogen Utilization Potential in Subsurface Sediments. *Front. Microbiol.* 7:8. doi: 10.3389/fmicb.2016.00008

Subsurface microbial communities undertake many terminal electron-accepting processes, often simultaneously. Using a tritium-based assay, we measured the potential hydrogen oxidation catalyzed by hydrogenase enzymes in several subsurface sedimentary environments (Lake Van, Barents Sea, Equatorial Pacific, and Gulf of Mexico) with different predominant electron-acceptors. Hydrogenases constitute a diverse family of enzymes expressed by microorganisms that utilize molecular hydrogen as a metabolic substrate, product, or intermediate. The assay reveals the potential for utilizing molecular hydrogen and allows qualitative detection of microbial activity irrespective of the predominant electron-accepting process. Because the method only requires samples frozen immediately after recovery, the assay can be used for identifying microbial activity in subsurface ecosystems without the need to preserve live material. We measured potential hydrogen oxidation rates in all samples from multiple depths at several sites that collectively span a wide range of environmental conditions and biogeochemical zones. Potential activity normalized to total cell abundance ranges over five orders of magnitude and varies, dependent upon the predominant terminal electron acceptor. Lowest per-cell potential rates characterize the zone of nitrate reduction and highest per-cell potential rates occur in the methanogenic zone. Possible reasons for this relationship to predominant electron acceptor include (i) increasing importance of fermentation in successively deeper biogeochemical zones and (ii) adaptation of H₂ases to successively higher concentrations of H₂ in successively deeper zones.

Keywords: hydrogenase, tritium assay, deep biosphere, microbial activity, Lake Van, Barents Sea, Equatorial Pacific, Gulf of Mexico

INTRODUCTION

Microorganisms in subsurface environments compete for electron donors and acceptors as they do in most surface environments (D'Hondt et al., 2002). Availability of electron donors and acceptors usually decreases with sediment depth (Froelich et al., 1979; Middelburg, 1989). The predominant terminal electron acceptor is typically inferred to change with sediment depth (e.g., Froelich et al., 1979), with reduction of dissolved O₂, NO₃⁻, Mn⁴⁺, Fe³⁺, and SO₄²⁻ predominating at successively greater depths. After these oxidants are largely exhausted, only fermentation and methanogenesis are left to degrade organic matter (Martens and Berner, 1974; Froelich et al., 1979).

This standard model often provides a good first-order description of the vertical succession of principal terminal electron-accepting activities. However, several studies have shown that multiple organic matter-degrading processes (SO_4^{2-} reduction, metal reduction, and methanogenesis) co-exist in the same depth intervals of deep seafloor sediment (e.g., Mitterer et al., 2001; D'Hondt et al., 2002, 2004, 2014; Wang et al., 2008; Holmkvist et al., 2011). Some of these studies show that methanogenesis occurs in zones where sulfate-reduction is the predominant terminal electron acceptor (Mitterer et al., 2001; D'Hondt et al., 2002, 2004, 2014; Wang et al., 2008), while others show that iron reduction occurs deep in the sulfate-reducing zone (Wang et al., 2008; D'Hondt et al., 2014) or that sulfate reduction occurs deep in the "methanogenic" zone (Holmkvist et al., 2011). These deviations from the generally assumed order of electron acceptor utilization represent a significant challenge when trying to quantify microbial activity in subsurface sediment.

These depth-dependent changes in predominant electron acceptor and the overlap of different electron-accepting processes pose challenges for attempts to identify and quantify microbial activity in the sediment column (Wang et al., 2008; Teske, 2012). Currently, there are two general approaches to assess microbial activity across different predominant electron-accepting regimes: (i) separately determine rates of different individual processes and convert them to a common currency (e.g., number of carbon atoms oxidized or electrons transferred; Canfield et al., 1993; D'Hondt et al., 2004) or (ii) measure a parameter that is widely distributed but independent of any specific metabolic process.

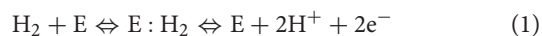
The situation is further complicated by the fact that some measurements quantify potential activities (e.g., by measurement of *ex situ* rates) while others quantify actual *in situ* activities. Potential rates of some specific processes, e.g., SO_4^{2-} reduction and anaerobic oxidation of methane (AOM) can be quantified with high sensitivity through radiotracer experiments (Kallmeyer et al., 2004; Treude et al., 2005). Potential rates of other processes, such as denitrification, can be quantified using stable isotope tracers (review in Bedard-Haughn et al., 2003).

Several approaches have been made in recent years to develop measures of microbial activity that can be used regardless of terminal electron acceptor (references in Adhikari and Kallmeyer, 2010). Promising approaches include measurements of hydrogenase (H_2 ase) enzyme activity (Schink et al., 1983) and adenosine triphosphate (ATP) concentration (Vuillemin et al., 2013). In a sense, both of these approaches measure potential rates, since they typically rely on measurement of concentration or *ex situ* activity in recovered samples. Soffientino et al. (2006) developed a method for quantifying H_2 ase activity by using a tritium-based H_2 ase assay. This technique has been successfully applied in several studies of subsurface sediment (Soffientino et al., 2006, 2009; Nunoura et al., 2009).

Hydrogen is a key component in anaerobic metabolism and it plays an important role in many biogeochemical reactions (Hoehler et al., 1998; Jørgensen et al., 2001; Nealson et al., 2005). Molecular H_2 is an important product of fermenters (Laanbroek and Veldkamp, 1982), a byproduct of the nitrogenase reaction by nitrogen-fixing bacteria (Dixon, 1978) as well as a substrate for methanogens (Zeikus, 1977) and sulfate reducers (Jørgensen,

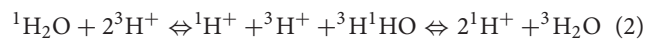
1978b). Several studies have shown that H_2 is a controlling factor for microbial activity in subsurface environments (Stevens and McKinley, 1995; Anderson et al., 2001; Nealson, 2005; Spear et al., 2005; Hinrichs et al., 2006). Despite the importance of molecular H_2 in microbial ecosystems, it is rarely quantified in sediment studies, mainly due to technical challenges associated with sampling and sample preservation, measurement of very low concentrations, and potentially high H_2 turnover rates (Hoehler et al., 2001). In addition to biotic processes, H_2 can be generated in the subsurface by alteration of young basaltic crust (Stevens and McKinley, 1995; Bach and Edwards, 2003) and by radiolysis of water (Holm and Charlou, 2001; Lin et al., 2005; Blair et al., 2007).

Hydrogenases are intracellular enzymes present in a wide range of microbes (Schink et al., 1983; Vignais and Billoud, 2007). Because hydrogenases facilitate H_2 utilization and production regardless of terminal electron acceptor, quantification of H_2 ase activity could provide an estimate of microbial activity regardless of predominant terminal electron-acceptor or co-occurrence of different terminal electron acceptors. During the catalytic conversion of H_2 , protons and electrons are produced or consumed based on thermodynamic constraints. Thereby cellular metabolism is facilitated, for example proton gradient formation in the cell membrane to synthesize ATP (Odom and Peck, 1984). Microbes utilize the available electrons from the oxidation of the electron donors to reduce the electron acceptors. The excess energy of this process is harvested through maintaining the proton gradient required for ATP synthesis by which the energy of the catabolic reaction is finally stored in ATP, representing the energy currency in any living cell.

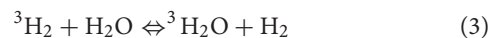


where, E is H_2 ase enzyme and E: H_2 is the reduced intermediate H_2 ase enzyme complex.

Other enzymes like ATPases and hydrolases are also involved in the pumping of protons; they can also split water molecules to facilitate hydrolytic reactions, however, they are not able to convert molecular H_2 into protons and electrons. H_2 ase enzymes activate H_2 molecules by heterolytic cleavage, which is the oxidation of hydrogen to protons (Equation 1). When incubating the sample with tritium, the generated $^3\text{H}^+$ will result in the formation of tritiated water (Equation 2).



The overall reaction will be as follows (Equation 3)



Measurement of the increase of radioactivity of the water can thus be used to infer the rates of hydrogen oxidation catalyzed by the hydrogenase enzymes. According to the modified Michaelis-Menten equation for the reaction shown in Equation (1), by incubating the sample with an excess of molecular H_2 , the forward reaction is strongly favored (Schink et al., 1983) and the backward reaction becomes essentially negligible for the

tritium-based assay (Soffientino et al., 2006). Due to the large excess of molecular H₂, neither its concentration nor the specific activity of ³H₂ (activity of the radioactive substance per mole of total reactant) will significantly change during the course of the incubation, which is a prerequisite for any rate measurement with a radiotracer (Fossing, 1995). The increase in ³H₂O over time yields a rate of ³H⁺ generation that is proportional to the total potential activity of all present H₂ase enzymes. Another factor that strongly favors the forward reaction, i.e., the oxidation of ³H₂ to ³H₂O, is the dilution of the produced ³H₂O in the large H₂O pool, thereby effectively removing the product.

Different metabolic processes involve different amounts of H₂ and utilize different types and numbers of H₂ases with different exchange rates. Moreover, different processes occur simultaneously and their respective contributions to total H₂ turnover are not known. Consequently, it is essentially impossible to translate hydrogen oxidation into specific metabolic rates. However, it may be possible to identify broad relationships between hydrogen oxidation rates and predominant terminal electron acceptors by comparing H₂ase activities of sedimentary regimes with different predominant electron acceptors. To test for such relationships, we measured potential H₂ oxidation in sediment cores from different environments in which different electron acceptors were quantitatively most important. Additionally, we calculated the net turnover rate of the quantitatively most important terminal electron-accepting process. We compared the different datasets to evaluate whether the measured potential hydrogen oxidation rates show any relationship to predominant terminal electron acceptors.

MATERIALS AND SITES DESCRIPTION

Investigation of different lacustrine and marine sedimentary environments allows testing of the general applicability of the H₂ase assay in various subsurface environments. We therefore obtained a set of samples that cover a wide range of environments and represent different predominant electron acceptor regimes. We chose the four sampling areas based on sample and data availability, because we needed access to (i) suitable samples for hydrogen oxidation measurements, (ii) porewater chemistry data, and (iii) cell abundance data.

Lake Van, Turkey

Lake Van, one of the largest soda lakes on Earth (Kadioglu et al., 1997), is located in Eastern Anatolia, Turkey. It covers an area of 3570 km² and has a maximum water depth of 460 m (Litt et al., 2009). Bottom water temperature is ca. 3°C (Litt et al., 2012). The lake water has an alkalinity of 155 mEq L⁻¹ and a pH of ca. 10, which is mainly due to evaporation and to weathering of nearby volcanic rocks (Kempe et al., 1991). The lake consists of two major basins, which are separated by basement highs and ridges (Figure 1). The Northern Ridge separates the smaller and shallower Northern Basin (NB) from the main Tatvan Basin. Ahlat Ridge (AR) is a small ridge bordering the Ahlat Subbasin, which is located between the NB and the Tatvan Basin. We collected sediment cores during the International Continental Scientific Drilling Program (ICDP) PaleoVan Drilling Operation

in summer 2010. For our study, we used short gravity cores of ca. 0.8 m length from the Northern Basin and Ahlat Ridge, taken at water depths of 260 and 375 m, respectively.

Barents Sea

The Barents Sea is located between the Norwegian Sea to the southwest and the Arctic Ocean to the north. The sampling area is located between the southwestern part of the Loppa High and Ringvassøy-Loppa fault complex (Figure 1). Samples were collected during a 2010 cruise onboard M/S HU Sverdrup II (Nickel et al., 2012). The morphology of the seabed in the sampling area is peculiar as it contains an average of ca. 100 pockmarks per square kilometer. The randomly distributed pockmarks are thought to have been formed by sudden expulsion of fluids or gas from the sediment (Solheim, 1991). The currently inactive pockmarks have a diameter of 10–50 m and an average depth of 1–3 m. Average water depth in the investigated area is around 350 m. Bottom water temperature was around 5°C (Nickel et al., 2012). The samples were retrieved from short gravity cores of ca. 1.5–1.8 m length taken inside the pockmarks at B1 and B9 locations (Nickel et al., 2012).

Equatorial Pacific

We retrieved samples during the early 2009 R/V Knorr Cruise 195-III in the eastern and equatorial Pacific upwelling area. This region has high primary productivity of ca. 15 mmol C m⁻² year⁻¹ (Røy et al., 2012). Water depths at sites EQP-05 and EQP-07 are 4394 and 4314 m, respectively (Figure 1). Bottom water temperature is approximately 2°C. Using the long core system from the Woods Hole Oceanographic Institution (WHOI), we recovered sediment cores with a maximum length of 35 m.

Gulf of Mexico

Sediment cores were retrieved during IODP Expedition 308 using an advanced piston corer (APC) and an extended core barrel (XCB). Samples were collected from two sites (U1319 and U1320) at the Brazos-Trinity (BT) Basin and two sites (U1322 and U1324) at the Mars-Ursa Basin (Figure 1) (Flemings et al., 2006). Temperatures of the samples ranged from 4 to 10°C, depending on sediment depth (Long et al., 2008). Volumetric H₂ase activity and cell abundance data are already published (Nunoura et al., 2009) and we obtained all other geochemical data from the IODP database (<http://iodp.tamu.edu/janusweb/general/dbtable.cgi>). Porewater extraction, sulfate, and CH₄ analyses of IODP Expedition 308 samples were carried out on board according to standard IODP protocols (Flemings et al., 2006).

METHODS

Porewater Extraction

Porewater was extracted with an IODP-style titanium/PTFE porewater extraction system (Manheim, 1966) in a hydraulic press (2-column bench top laboratory press, 22 ton max load, Carver Inc., USA). The porewater was filtered through syringe filters (pore size: 0.45 μm) and either analyzed immediately or stored frozen until analysis. During previous expeditions,

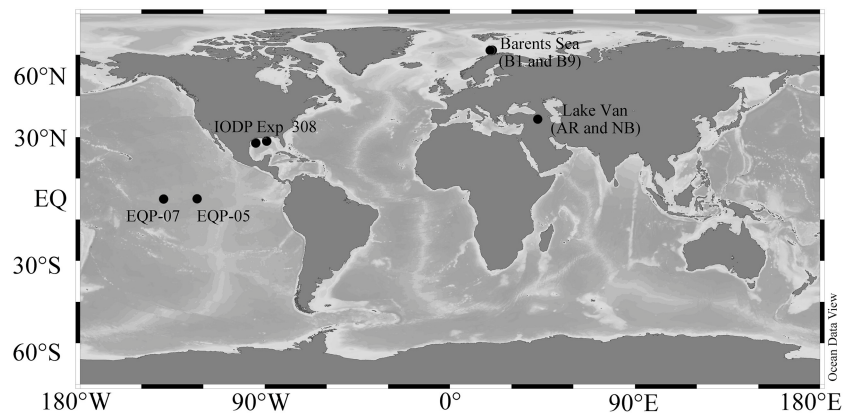


FIGURE 1 | Study Sites. The sampling locations Lake Van (AR and NB), Barents Sea (B1 and B9), Equatorial Pacific Sites (EQP-05 and EQP-07), and IODP Expedition 308 Gulf of Mexico (Brazos-Trinity and Ursa Basin) drilling regions plotted in a map using Ocean Data View (<http://odv.awi.de/>).

it was shown that porewater extraction by sediment squeezing generates NO_3^- concentrations on the scale of tens of micromoles (Schrum et al., 2012). Thus, NO_3^- concentrations in the porewater samples obtained during the equatorial Pacific expedition were measured in samples obtained using Rhizon soil moisture samplers (Seeberg–Elverfeldt et al., 2005). This practice allowed us to effectively quantify very low NO_3^- concentrations ($<1 \mu\text{mol L}^{-1}$).

Porewater Analyses

Nitrate

During the Equatorial Pacific expedition, NO_3^- concentrations were analyzed with a Metrohm 844 UV/VIS Compact IC equipped with a $150 \times 4.0 \text{ mm}$ Metrosep A SUPP 8 150 column. The column temperature was set to 30°C . The eluent was a 10% NaCl solution filtered through a $0.45 \mu\text{m}$ pore size filter. Approximately 0.8 ml of interstitial water was injected manually into a $250 \mu\text{L}$ sample loop. UV absorption was determined at 215 nm .

Mn and Fe

We analyzed porewater samples for dissolved Mn^{4+} and Fe^{3+} by inductively coupled plasma emission spectrometry (ICP-ES) at Boston University. We acidified the samples at sea with Fisher Optima HNO_3 and stored them in a refrigerator until analysis. The samples were diluted 10-fold in 2% triple distilled HNO_3 , and calibrated against a seven point calibration curve of matrix matched, spiked International Association for the Physical Sciences of the Ocean standard seawater (IAPSO, $S = 35$, Ocean Scientific International Ltd.) that covered the full concentration range of the unknown samples. We measured Mn^{4+} at 257.609 and 259.373 nm using the ICP-ES monochromator and at 257.61 nm using the ICP-ES polychromator with the Jobin-Yvon Ultima C ICP-ES instrument. Using the ICP-ES monochromator, we measured Fe^{3+} at 238.203 and 259.939 nm , as well as at 259.94 nm using the ICP-ES polychromator. We corrected final concentrations for the 1% acid dilution due to on-board acidification. Analytical precision for both elements is $\sim 3\%$ of

the measured value. Accuracy was confirmed by analysis of spiked IAPSO standards that were not included in the original calibration.

Sulfate

We quantified dissolved SO_4^{2-} in porewater samples from Lake Van and Barents Sea samples using a SYKAM IC system (SYKAM, Fürstenfeldbrück, Germany) equipped with an LCA A14 column, a suppressor (SAMSTM, SeQuant, Sweden) and a S3115 conductivity detector. The mobile phase was a 6.25 mmol L^{-1} Na_2CO_3 with 0.1 vol% modifier (1g 4-hydroxybenzonitrile in 50 mL methanol). We eluted the samples at isocratic conditions at 50°C with the eluent flow set to 1 mL min^{-1} , injection volume was $30 \mu\text{L}$.

During the Equatorial Pacific expedition, we quantified SO_4^{2-} concentrations with a Metrohm 861 Advanced Compact IC. The IC was comprised of an 853 CO_2 suppressor, a thermal conductivity detector, a $150 \times 4.0 \text{ mm}$ Metrosep A SUPP 5 150 column, and a $20 \mu\text{L}$ sample loop. A Metrohm 837 IC Eluent/Sample Degasser was coupled to the system. We set the column oven to 32°C . The eluent was 3.2 mmol L^{-1} Na_2CO_3 , and 1.0 mmol L^{-1} NaHCO_3 . Each sample was analyzed as a 1:50 dilution of interstitial water with 18 MOhm cm^{-1} deionized water. If the samples were anoxic, we added $5 \mu\text{L}$ of 10% Zn-acetate per mL of analyte to precipitate ZnS .

Cell Enumeration

We took samples for cell enumeration immediately after each core was retrieved. Using cut-off plastic syringes, we placed 2 cm^3 subsamples in a 15 mL centrifuge tube containing 8 mL of either seawater or NaCl solution with a concentration corresponding to the salinity of the sample. Both solutions were $0.2 \mu\text{m}$ -filtered and contained 2% formalin as a fixative. We shook the tubes vigorously to create homogenous slurries and stored them at 4°C until analysis.

We undertook cell counts by either (i) direct cell counting or (ii) in cases where cell counts fell below the minimum detection limit of the direct counts, using the cell extraction protocol of

Kallmeyer et al. (2008). In cases where cell extraction became necessary, e.g., in deeper sediment layers, we used the two methods with some overlap, to assess the extraction efficiency of the cell separation. In all cases, the two types of counts deviated by less than one standard deviation based on triplicates.

We filtered the sediment slurry or the separated cells onto polycarbonate filters (pore size: $0.2\ \mu\text{m}$) stained with SYBR Green I according to Morono et al. (2009) and counted the cells using epifluorescence microscopy. Cell counts of samples from IODP Expedition 308 are from Nunoura et al. (2009). For Expedition 308, a 1 mL sediment sample was fixed in 9 mL of 3.7% formaldehyde with PBS and stored in 1:1 (v/v) ethanol:PBS solution. Subsamples were filtered on a polycarbonate membrane, stained with both AO and DAPI, and enumerated by epifluorescence microscopy.

Modeling of Net Turnover Rates Based on Porewater Concentration Profiles

We modeled net turnover rates of predominant terminal electron acceptors using porewater concentration profiles and the approach of Wang et al. (2008). In brief, we smoothed the porewater concentration profiles of predominant terminal electron acceptors with a 5-point Gaussian filter. We used each smoothed concentration profile as an input parameter to model the reaction rate of the profiled chemical by applying the MATLAB[®] script of Wang et al. (2008). For these calculations, we used a constant formation factor, as well as constant diffusivity and porosity. In addition, we applied a constant sedimentation rate and constant external flow advection velocity near the sediment-water interface. We used a minimum of three concentration data to determine each reaction zone. Modeling of substrate turnover rates from porewater concentration profiles is generally not applicable for near-surface sediment due to disturbance of the sediment-water interface by various factors (e.g., impact of the coring device, bioturbation, etc.; see Jørgensen, 1978a). Thus, the calculated results for the upper meter should be considered carefully. At Lake Van, data from the shallowest samples should still be useful, as anoxic bottom water precludes bioturbation there, and the small coring device that was used probably had little impact on sediment structure (Glombitza et al., 2013). The results of these calculations include positive and negative turnover rates for different depth intervals, with positive rates indicating production of the respective chemical and negative rates indicating consumption. The script of Wang et al. (2008) fixes the modeled concentration at the top and bottom to the uppermost and lowermost measured values. This forcing may cause arbitrary turnover profiles in cases where the measured values show high scatter.

Hydrogenase Enzyme Assay

We used a tritium-based H_2 ase assay to measure the potential oxidation rates of hydrogen (Soffientino et al., 2006). We took whole round core pieces or subsamples from the center of each core with cut-off syringes immediately after core retrieval, packed the pieces or subsamples in gas-tight aluminum bags flushed with nitrogen gas, and froze them immediately at -80°C until analysis.

Headspace Preparation

We diluted the carrier-free radioactive $^3\text{H}_2$ (American Radiolabeled Chemicals, Inc.) because its specific activity was too high ($37\ \text{GBq mL}^{-1}$) to allow for safe and reproducible handling. We prepared the $^3\text{H}_2$ headspace gas by mixing the carrier-free $^3\text{H}_2$ gas with a non-radioactive (20/80% H_2/N_2) gas according to Soffientino et al. (2009), considering H_2 ase half-saturation constants and specific activity of $^3\text{H}_2$ (amount of radioactivity per mole of H_2) to be high enough for sufficient measurement sensitivity when using a slurry to headspace ratio of 1:3. Higher H_2 concentrations would reduce the specific activity of the $^3\text{H}_2$. To store, dilute and dispense the gas, we constructed a manifold (Figure 2) according to Soffientino et al. (2009) with some minor modifications. In brief, the manifold consists of a 1 L stainless steel cylinder (Figure 2A) for storage of $37\ \text{GBq}$ of $^3\text{H}_2$ gas in a mixture of non-radiolabeled 20% H_2 and 80% N_2 (Figure 2B). The cylinder is connected to the headspace reservoir bag (Figure 2C) via a stainless steel loop with a volume of 11.4 mL (Figure 2D). To prepare the desired specific activity of $^3\text{H}_2$, we diluted one or several volumes of the loop with known volumes of non-radioactive gas. Unlike Soffientino et al. (2009), we added an O_2 scrubber (Figure 2E) to remove traces of O_2 from the diluent gas before it is mixed with the $^3\text{H}_2$. The O_2 scrubber consists of two graduated cylinders filled with chromous chloride (CrCl_2) solution produced by reacting 1 mol L^{-1} $\text{CrCl}_3 \cdot 6\text{H}_2\text{O}$ in 0.5 mol L^{-1} HCl with Zn granules under a stream of N_2 (Zhabina and Volkov, 1978). The top of the first cylinder is connected to a non-radiolabeled H_2/N_2 gas tank and the stainless steel loop via a three-way valve. Gas entering the cylinder from the tank replaces the CrCl_2 solution. Through an outlet at the bottom, the gas flows into the second glass cylinder that is connected to a gas-tight aluminum bag (Figure 2F) filled with N_2 gas to maintain O_2 -free conditions and allow for volume changes. In addition to serve as O_2 scrubbers, the graduated cylinders were also used to measure the volume of dilution gas. We then flushed the desired volume of non-radioactive gas through the stainless steel loop into the reservoir bag. Finally, we filled the glass syringes with the diluted $^3\text{H}_2$ gas via a sample port (Figure 2G).

We measured specific activity of the headspace gas as described by Soffientino et al. (2009). In brief, we reacted 500- μL $^3\text{H}_2/\text{N}_2$ gas with air in the presence of a heated platinum catalyst to form $^3\text{H}_2\text{O}$ in a Knallgas-reactor. We trapped the $^3\text{H}_2\text{O}$ with 5 mL distilled water and quantified radioactivity of the $^3\text{H}_2\text{O}$ by liquid scintillation counting.

Sample Preparation

For the measurement of potential hydrogen oxidation rates, we placed ca. 2 g of frozen sediment into a 50 cm^3 glass syringe barrel fitted with a three-way stopcock and mounted vertically on a manifold. The sediment had to be slurried, so we added 10 mL of sterile anoxic NaCl solution at the concentration necessary to maintain *in situ* salinity in each sample. In order to prevent O_2 contamination, we performed the process under a continuous stream of N_2 . We processed each sample in triplicates, along with a negative control treated with 0.5 mL saturated HgCl_2 solution. We incubated all four slurries with 30 cm^3 headspace

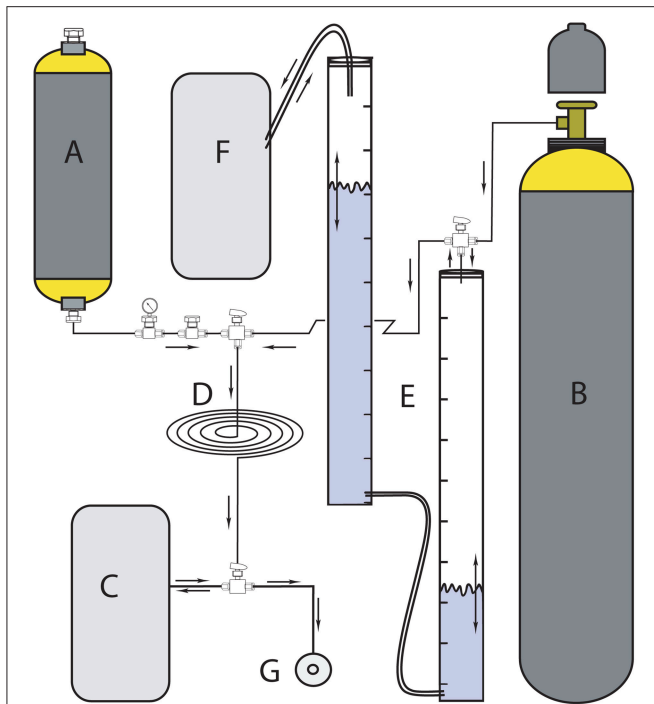


FIGURE 2 | Headspace $^3\text{H}_2/\text{N}_2$ manifold for storing, diluting, and dispensing $^3\text{H}_2$ gas to the incubation syringes (modified after Soffientino et al., 2009). (A) 1-L stainless steel cylinder filled with 37 GBq stock $^3\text{H}_2$ gas; (B) cold gas mixture reservoir (20% H_2 in N_2); (C) secondary headspace reservoir; (D) tubing loop; (E) two measuring cylinders filled with CrCl_2 solution to remove traces of O_2 contained in cold gas mixture before headspace preparation; (F) pressure maintaining bag during O_2 removal, and (G) headspace port.

gas ($^3\text{H}_2$ mixed with non-radioactive 20/80% H_2/N_2) on a shaker at 250 rpm at room temperature (ca. 25°C). We collected five subsamples of ca. 0.5 mL at 0.5, 1, 2, 3, and 4 h from each of the slurries and removed unreacted $^3\text{H}_2$ gas by flushing the subsample with N_2 gas for 10 min and remaining sediment particles by centrifugation. We mixed 100 μL of supernatant with 4 mL Perkin Elmer[®] Ultima Gold LLT scintillation cocktail for radioactivity quantification by liquid scintillation counting on a Perkin Elmer TriCarb TR2800. The slope of the linear regression over the increase in radioactivity with time is a measure of the potential H_2ase activity. The killed control should not show any slope and helps to identify abiotic processes that mimic H_2ase activity (e.g., minerogenic splitting of water molecules).

RESULTS

Using the calculation approach of Soffientino et al. (2006), we quantified potential hydrogen oxidation in all samples from all depths. However, the rates vary significantly between sites and depths. Our killed control experiment shows no positive slope (no $^3\text{H}_2$ incorporation into water) over time. The error bars (Figures 3, 4) represent one standard deviation calculated from the replicates.

Lake Van

At the Ahlat Ridge (AR) site, we found minimum potential hydrogen oxidation rates of $3.60 \pm 1.08 \mu\text{mol H}_2 \text{ cm}^{-3} \text{ d}^{-1}$ in the uppermost layer [0.03 m below lake floor (mblf)]. Potential rates initially increases with sample depth, reaching a maximum of $17.85 \pm 3.07 \mu\text{mol H}_2 \text{ cm}^{-3} \text{ d}^{-1}$ at a depth of 0.43 mblf, before decreasing again to $11.60 \pm 1.98 \mu\text{mol H}_2 \text{ cm}^{-3} \text{ d}^{-1}$ at the bottom of the core (0.72 mblf). At the Northern Basin (NB) site, potential hydrogen oxidation rates decreases with depth. In the uppermost sediment layer (0.01 mblf), we observed maximum activity of $2.42 \pm 0.60 \mu\text{mol H}_2 \text{ cm}^{-3} \text{ d}^{-1}$. Despite some scattering the potential rates at the NB site decreases by an order of magnitude within a few centimeters and remains in the range of $0.20\text{--}1.20 \mu\text{mol H}_2 \text{ cm}^{-3} \text{ d}^{-1}$ between 0.14 and 0.74 mblf (Figure 3).

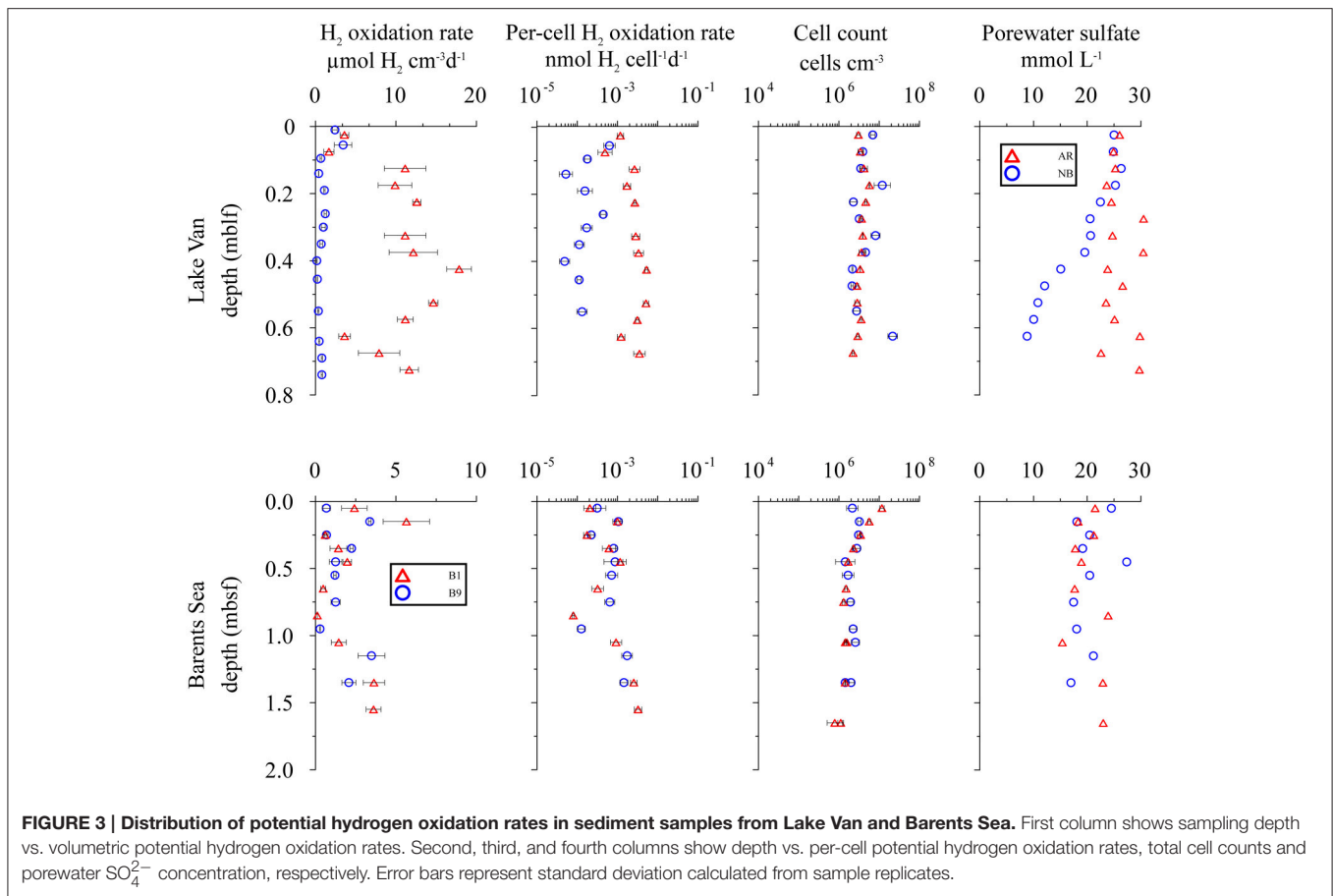
At AR, microbial cell numbers are constant around 10^6 cells cm^{-3} and show little variation with depth. The cell numbers at NB are roughly in the same range but show higher scatter (Figure 3; Kallmeyer et al., 2015). At both sites, pore water SO_4^{2-} concentration in the uppermost sediment layer is ca. 26 mmol L^{-1} . While at the NB site, concentrations decrease almost linearly to 8 mmol L^{-1} at 0.65 mblf, they remain constant throughout the core, with some scatter at the AR site. In cores from both sites, Glombitza et al. (2013) measured microbial SO_4^{2-} reduction rates in radiotracer incubations ($^{35}\text{SO}_4^{2-}$). At AR, the radiotracer-based rates are uniformly around $2 \text{ nmol cm}^{-3} \text{ d}^{-1}$, whereas at NB, rates drop from $>20 \text{ nmol cm}^{-3} \text{ d}^{-1}$, at the surface to $2 \text{ nmol cm}^{-3} \text{ d}^{-1}$ at 0.2 mblf.

The correlations (R^2) between measured and modeled sulfate concentrations are 0.59 and 0.98 for AR and NB, respectively. The high scatter of the pore water SO_4^{2-} data causes the much lower correlation coefficient for AR, although we excluded a few data points because they fall well outside of the general trend and are probably erroneous measurements. Thus, the calculated rates have to be treated with caution (Figure 6). Still the calculated *in situ* reaction rates show that sulfate reduction occurs in parts of the sediment cores from both sites, with maximum rates of $2.2 \text{ nmol cm}^{-3} \text{ d}^{-1}$ and $4.9 \text{ nmol cm}^{-3} \text{ d}^{-1}$ at AR and NB, respectively. For both sites, calculated depth intervals of sulfate production may be an artifact of either high data scatter (AR) or advective exchange of solutes in the uppermost sediment column.

We could not detect nitrate in the porewater. This is not surprising because the bottom water is anoxic (Kaden et al., 2010) and NO_3^- concentrations are below $1 \mu\text{mol L}^{-1}$ throughout the water column (Reimer et al., 2009). Methane was below the detection limit of about $0.06 \mu\text{mol L}^{-1}$ in all samples.

Barents Sea

Potential hydrogen oxidation rates at both sites in the Barents Sea (B1, B9) vary between 0.12 and $5.65 \pm 2.88 \mu\text{mol H}_2 \text{ cm}^{-3} \text{ d}^{-1}$ (Figure 3). Except for the two uppermost samples, where cell counts of site B1 are higher by up to an order of magnitude, they are almost identical at both sites and vary with depth from 10^6 to 10^7 cells cm^{-3} . At both sites, SO_4^{2-} concentration is around 20 mmol L^{-1} throughout the cores and shows considerable scatter. The SO_4^{2-} profiles indicate that microbial SO_4^{2-} reduction is very low over the depth interval covered by the cores. We



calculated *in situ* net reaction rates from combined sulfate data from both sites. Correlation between measured and smoothed sulfate concentrations is relatively low ($R^2 = 0.62$). Except for the uppermost 25 cm, where the calculated rate is $4.01 \text{ nmol cm}^{-3} \text{ d}^{-1}$ (Figure 6), the rates are around zero or even positive, which is in agreement with *in situ* rates measured in close vicinity to our sample sites. (Nickel et al., 2012) found very low sulfate reduction rates of $<100 \text{ pmol cm}^{-3} \text{ d}^{-1}$. We could not detect nitrate or CH_4 in these cores.

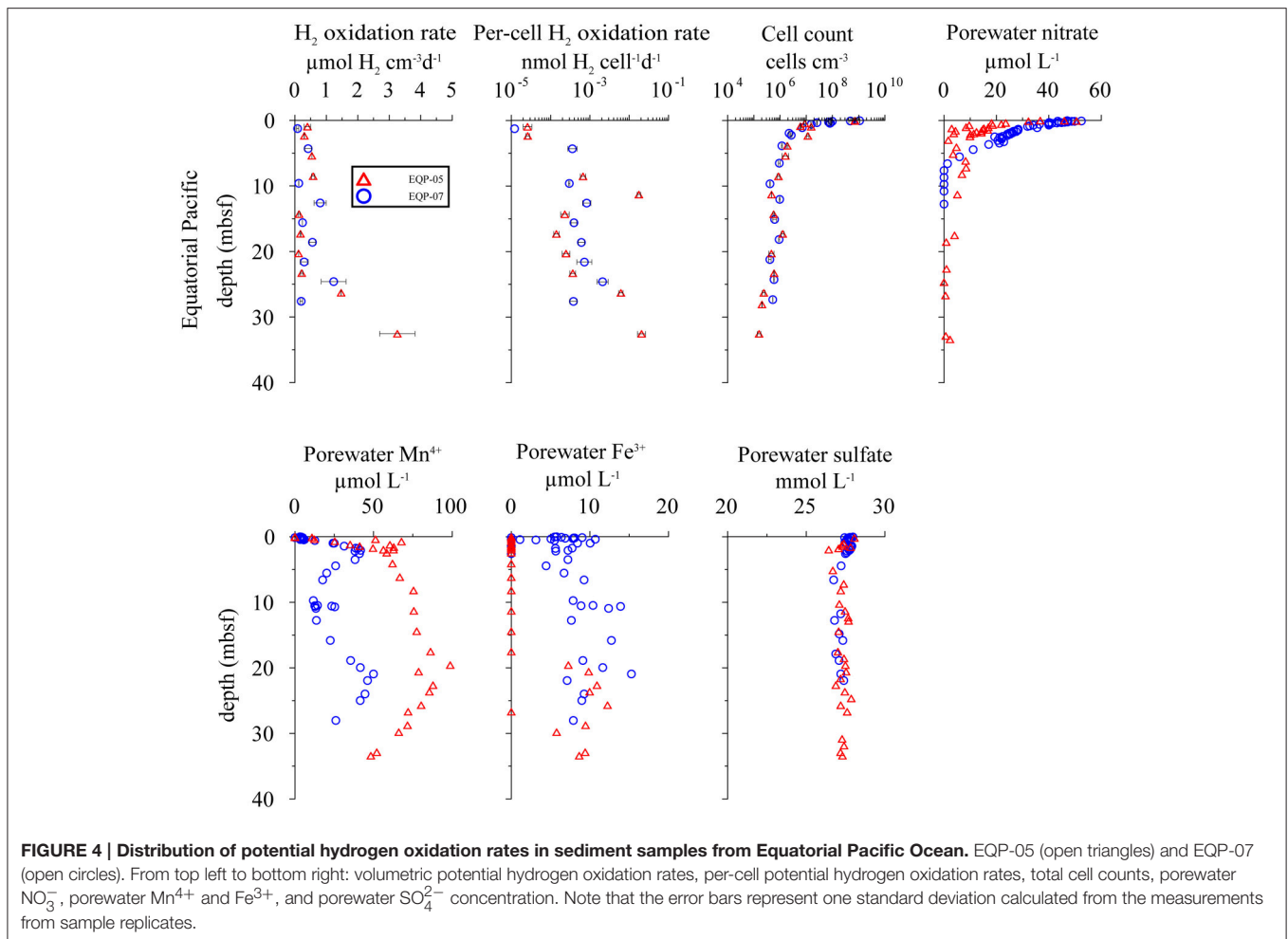
Equatorial Pacific Ocean

At both EQP sites, potential hydrogen oxidation rates are relatively low, with values between 0.08 ± 0.07 and $3.26 \pm 1.13 \text{ } \mu\text{mol H}_2 \text{ cm}^{-3} \text{ d}^{-1}$. We observed a slight increase in rates in the lowermost samples of EQP-05 (Figure 4). Cell abundance is up to $10^9 \text{ cells cm}^{-3}$ in the uppermost sediment layer (two to three orders of magnitude higher than in the other sediment analyzed for this study). Cell numbers decrease exponentially and remain between 10^5 and $10^6 \text{ cells cm}^{-3}$ at depths $>5 \text{ m}$ below sea floor (mbsf) at both EQP sites (Figure 4). Porewater SO_4^{2-} concentrations are near seawater values (28 mmol L^{-1}) through the entire cored interval. Consequently, the calculated reaction rates are near zero. Only in the uppermost sediment did we observe maximum SO_4^{2-} reduction rates of 4 and $109 \text{ pmol cm}^{-3} \text{ d}^{-1}$ for EQP-05 and EQP-07, respectively (Figure 6). At

EQP-05, the correlation between measured and smoothed SO_4^{2-} concentrations is very low ($R^2 = 0.38$), whereas at EQP-07 there is a better fit ($R^2 = 0.85$).

Nitrate is detectable with maximum concentrations of ca. $50 \text{ } \mu\text{mol L}^{-1}$ close to the sediment-water interface. Concentrations decrease steadily to the minimum detection limit of ca. $1 \text{ } \mu\text{mol L}^{-1}$ at around 2 and 7 mbsf at Sites EQP-05 and EQP-07, respectively (Figure 4). The strong decrease with depth and the little scatter of the pore water data allowed for good calculation of net nitrate reduction rates at both sites and the smoothed concentration data correlate very well with the measured data ($R^2 = 0.86$ and 0.99 for EQP-05 and EQP-07, respectively). For both sites, the calculation indicates nitrate production in the uppermost layer, followed by a zone of denitrification below. However, for most of the depth profile the calculated rates are very close to zero (Figure 6).

At EQP-05, Mn^{2+} concentration increases steeply over the upper 5 mbsf, from below detection to $67.75 \text{ } \mu\text{mol L}^{-1}$. Manganese concentrations further increase with a lower gradient to a maximum of $98.76 \text{ } \mu\text{mol L}^{-1}$ at 19.58 mbsf, and then steadily decrease with depth. Over the upper 3–4 mbsf of EQP-07, dissolved Mn^{2+} concentrations are almost identical to those at EQP-05. Below this depth they decrease to $11.73 \text{ } \mu\text{mol L}^{-1}$ at 9.73 mbsf before they increase again to a second maximum of $49.97 \text{ } \mu\text{mol L}^{-1}$ at 20.93 mbsf. The smoothed concentration



profile correlates very well with the measured data for Mn^{2+} at both sites ($R^2 = 0.91$ and 0.93). For EQP 5 calculated Mn^{2+} production in the uppermost meter is up to $2.5 \text{ pmol cm}^{-3} \text{ d}^{-1}$, followed by rates very close to zero at greater depths. For EQP7, the Mn^{2+} concentration profile looks quite different, and consequently also the calculated turnover rates. The strong change from almost -6 to $4 \text{ pmol cm}^{-3} \text{ d}^{-1}$ over the upper few centimeters is followed by rates very close to zero, changing back and forth between positive and negative values.

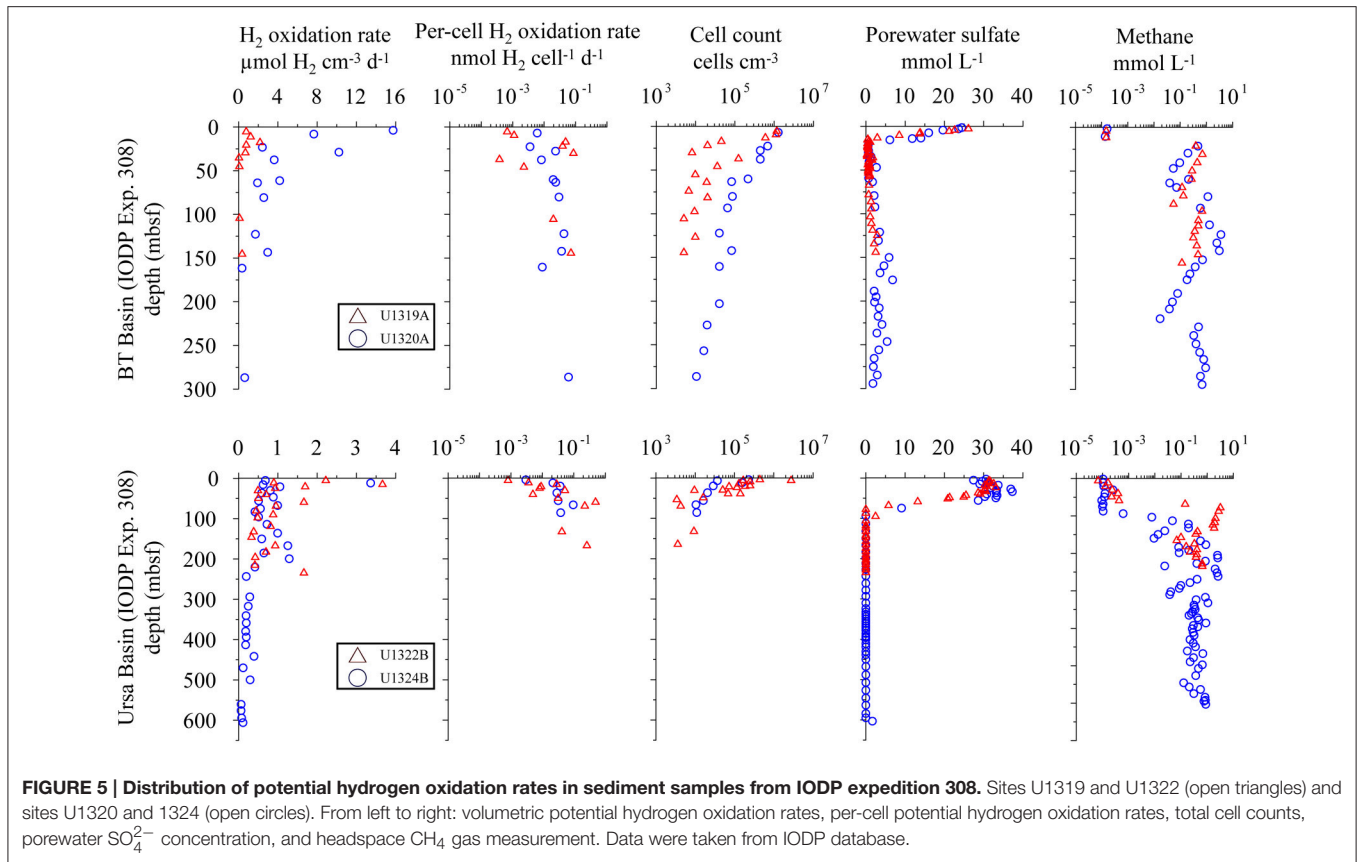
Dissolved Fe^{2+} concentrations show a different trend than Mn^{2+} . Dissolved Fe^{2+} concentrations at EQP-05 are below the detection limit until a depth of 17.52 mbsf, and then increase to a maximum of $10.90 \text{ } \mu\text{mol L}^{-1}$ at 22.64 mbsf. At EQP-07, dissolved Fe^{2+} concentration varies between 5 and $13 \text{ } \mu\text{mol L}^{-1}$ over the entire depth of the cored interval. There is a second maximum concentration peak at approximately the same depth at both sites. The smoothed Fe^{2+} concentration data correlate very well with the measured data at site EQP-05 ($R^2 = 0.83$), but poorly at EQP-07 ($r^2 = 0.52$). This poor EQP07 correlation is caused by the high scatter in Fe^{2+} data at EQP-07. Iron reduction rates for EQP-05 and EQP-07 are below $4.7 \text{ pmol cm}^{-3} \text{ d}^{-1}$ (Figure 6).

Gulf of Mexico

At all sites from IODP Expedition 308 (U1319, U1320, U1322, U1324), potential hydrogen oxidation rates are below $5 \text{ } \mu\text{mol H}_2 \text{ cm}^{-3} \text{ d}^{-1}$ at all depths, except for three samples from the upper 30 mbsf at site U1320 (Figure 5). These three samples show potential rates of up to $16 \text{ } \mu\text{mol H}_2 \text{ cm}^{-3} \text{ d}^{-1}$.

Cell counts are in the range of 10^6 – $10^7 \text{ cells cm}^{-3}$ close to the sediment-water interface and decrease to 10^3 – $10^4 \text{ cells cm}^{-3}$ at greater depth at all sites. The cell count profiles for sites U1322 and U1324 drop so rapidly below the minimum detection limit around $5 \times 10^3 \text{ cells cm}^{-3}$ that there are no cell count data for depth below 150 and 100 mbsf, respectively. Except for Site U1320, cell concentrations at all sites show high scatter, but decline more or less logarithmically with depth.

At Sites U1319 and U1320, dissolved SO_4^{2-} is completely depleted within the upper 10 mbsf, whereas at Sites U1322 and U1324, SO_4^{2-} concentration remains near seawater concentration in the upper 30 m and 50 m of sediment, respectively before dropping linearly and reaching the detection limit between 80 and 100 mbsf. The SO_4^{2-} profile is mirrored by the CH_4 concentration profile, with values between 0.62 and 6.2 mmol L^{-1} in the sulfate-free zone and low concentrations



($0.6 \mu\text{mol L}^{-1}$) where SO_4^{2-} is present. The sulfate-methane transition zone (SMTZ) can be identified at all four sites, but differs in depth below seafloor and thickness (Figure 5). Measured and smoothed SO_4^{2-} concentrations showed a very good correlation ($R^2 = 0.99$) at all sites (Figure 6). For SO_4^{2-} , the calculated turnover rates show similar profiles for U1319 and U1320, with a narrow subsurface maximum sulfate reduction zone of -7 and $-1.8 \text{ pmol cm}^{-3} \text{ d}^{-1}$, respectively, followed by near-zero values for the rest of the core. The calculated SO_4^{2-} turnover rates for U1322 and U1324 look considerably different, with more changes between positive and negative rates and a larger positive subsurface peak. The reason for this difference may partly be that the model fixes the concentration at top and bottom to the measured concentration, which may have led to arbitrary results for U1322. For U1324, there seems to be loss of SO_4^{2-} to the overlying water as concentrations in the upper 50–60 mbsf are higher than in the overlying water; this is rather unusual for marine sediments.

For CH_4 , we found reasonably good fits of measured concentrations to smoothed concentrations at Sites U1320A ($R^2 = 0.83$) and U1322B ($R^2 = 0.82$) and low correlations at Sites U1319A ($R^2 = 0.57$) and U1324B ($R^2 = 0.53$). The high scatter in the concentration data from the latter two sites prevents more accurate modeling and the results should be used with great caution. Still, zones of maximum activity can be identified.

DISCUSSION

Evaluation of the Hydrogen Oxidation Measurements

Our measurements only delivered potential rates as the conditions under which we performed the incubations differ in several ways from *in situ* conditions. Our use of previously frozen samples, slurries, room temperature, and excess headspace H_2 all cause deviation from *in situ* conditions.

We used previously frozen samples for all of our hydrogen oxidation measurements. Use of previously frozen material in incubation experiments is unusual for metabolic rate measurements. However, we are measuring potential hydrogen oxidation rates in the sediments, not metabolic activity. Although freezing samples prior to analysis might have damaged cells due to ice crystal formation, cellular integrity is of minor concern for this study; as long as the H_2 ase enzyme remains intact and it finds a redox partner like NAD or ferredoxin, it remains functional. If cells lyse, co-localization of redox partners may be perturbed, which would affect enzymatic rates. Consequently, the enzymes may be less likely to find such a partner in lysed cells than in intact cells. However, extracellular H_2 ases have been reported in soils (Häring et al., 1994), indicating that even extracellular enzymes may find such partners.

Little is known about the survival of H_2 ases outside of cells, as they have not been reported from aquatic or subsurface

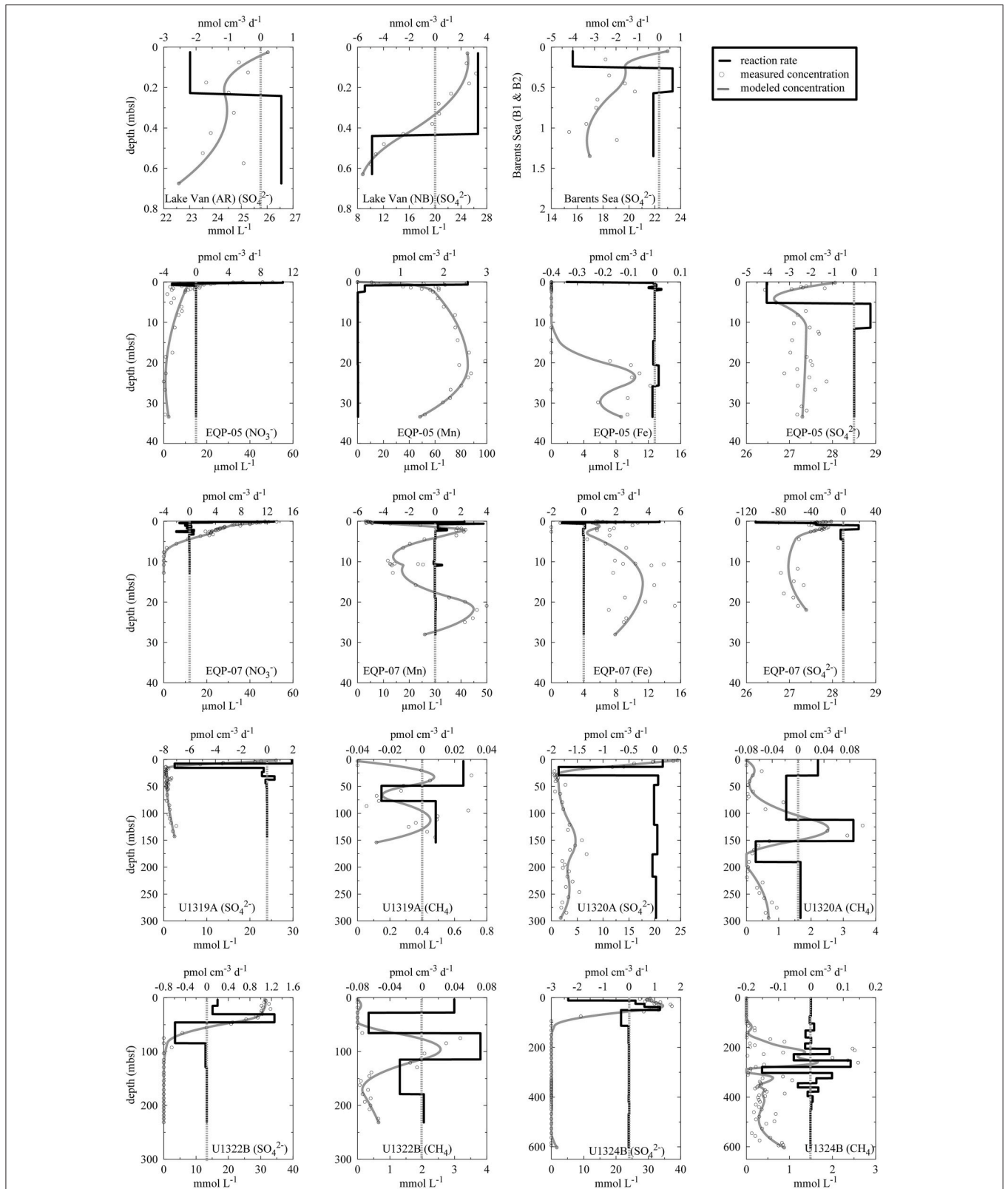


FIGURE 6 | Calculated reaction rates. Y-axis refers to depth in meter. Top and bottom x-axes refer to reaction rates and concentrations, respectively. Open circles are measured concentration data, gray solid lines are modeled concentrations, and dark solid lines are modeled reaction rates. Positive values refer to net production and negative values refer to net consumption. Please note different units on the x-axes. Note that the top and bottom values of the smoothed profiles are fixed to the upper- and lower-most measured values.

environments except soil. We therefore assume that all hydrogen oxidation catalyzed by hydrogenase enzymes is related to cells that were physiologically intact at the time of sampling. The samples were immediately frozen in a nitrogen atmosphere and thawed only inside the nitrogen-filled reaction vessel so degradation of biomolecules was minimized. Given the immediate freezing, storage, and thawing under nitrogen and the short incubation time, we assume that degradation of the enzyme is of minor concern, given the orders of magnitude variability of the normalized potential per-cell rates. The results of Soffientino et al. (2009) point toward the same interpretation. They assessed the effects of freezing and thawing on hydrogen oxidation and found 18% higher hydrogen oxidation in fresh sediment than in previously frozen samples, but also noted that more research would help to better constrain the effects of freezing. Due to the availability of only frozen samples, we could not run separate experiments on frozen and fresh material to evaluate this effect.

We made slurries for all of our incubations. Slurrying obviously disturbs sedimentary structure, which might have an effect on the potential turnover rates. Radiotracer SO_4^{2-} reduction-rate measurements done in slurries have resulted in higher rates than measurements made with intact sediment (Jørgensen, 1978b). Similar findings have been reported for AOM experiments (Treude et al., 2003, 2005). We therefore suspect that slurrying may have a similarly positive effect on our measured potential hydrogen oxidation rates.

We carried out our incubations at room temperature (ca. 25°C), which is considerably higher than *in situ* temperatures. Several studies have shown that increasing temperature has a positive effect on metabolic rates (Arnosti et al., 1998; Sagemann et al., 1998; Thamdrup and Fleischer, 1998; Finke and Jørgensen, 2008), usually leading to an increase by a factor of 3–5. One of the few studies that measured the temperature dependence of enzyme activity in sediments also found a ca. three to five-fold increase in polysaccharide hydrolysis between 5 and 25°C (Arnosti et al., 1998). Given the order-of-magnitude approach of our study we consider these changes to be negligible. Moreover, all samples have a relatively narrow *in situ* temperature range between 2 and 10°C, so the temperature effect should be similar in all samples.

Our most important deviation from *in situ* conditions is incubation of our sediment slurries with excess H_2 in the headspace (20%), leading to complete saturation of the samples with H_2 (ca. $16 \mu\text{mol L}^{-1}$), which is controlled by its solubility. In natural sedimentary systems, H_2 concentrations can be two to three orders of magnitude lower than in our incubations (e.g., Hoehler et al., 1998). Hoehler et al. (2002) showed that microorganisms can maintain H_2 concentrations at a thermodynamically favorable level, for example, SO_4^{2-} reducers maintain H_2 concentration at such a low level that conditions can become thermodynamically unfavorable for CO_2 reducers. By supplying excess H_2 , our experiments over-ride these naturally low concentrations and allow for unlimited H_2 oxidation with negligible back-reaction according to Michaelis-Menten kinetics (Soffientino et al., 2009; Equation 3). In short, our measurements provide rates of H_2 oxidation that are facilitated by H_2 ases regardless of the *in situ* direction of the process. Because

fermenters produce most of the H_2 that is used by other microbes, about half of the measured potential hydrogen oxidation should account for H_2 production under *in situ* conditions.

The excess of H_2 is necessary to ensure comparable conditions in all samples, because we do not have any information about *in situ* concentrations. Experiments under *in situ* temperature and H_2 partial pressure might provide results closer to *in situ* rates but incubating samples under high hydrostatic pressure and maintaining precise H_2 partial pressure entail additional technical challenges (Sauer et al., 2012) that are beyond the scope of this study. As shown by Soffientino et al. (2006), saturating the slurry with H_2 and constant shaking during the incubation is necessary to achieve a linear increase in the concentration of $^3\text{H}_2\text{O}$ (i.e., constant enzyme activity) because the reaction is diffusion-limited. The low solubility of H_2 in water (ca. $16 \mu\text{mol L}^{-1}$ at 25°C) is partially countered by its high diffusivity ($8.69 \times 10^{-9} \text{ m}^2 \text{ s}^{-2}$ at 25°C; Jørgensen, 2000, which is similar to the diffusivity of water ca. $2.5 \times 10^{-9} \text{ m}^2 \text{ s}^{-2}$ at 25°C), leading to a diffusion time of $<0.1 \text{ ms}$ for a distance of $1 \mu\text{m}$. This distance is larger than the diameter of an average microbial cell in subsurface sediment (Kallmeyer et al., 2012). Although intracellular membranes restrict diffusion to some degree, we think that it is safe to assume that all intracellular reactants are in equilibrium with the surrounding water over the time course of the experiment.

Volumetric potential hydrogen oxidation (H_2 turnover per volume sediment) varies by about two orders of magnitude between sites and depths, without any visible correlation with depth, sites, or biogeochemical zones. We interpret this as indicating that H_2 ases are ubiquitously distributed and a potentially active microbial community is present at all sampled depths at all sites in this study (Figures 3–5). Except for disruption of the cells due to freezing and the consequent potential loss of a redox partner (Soffientino et al., 2009), the deviations of our incubations from *in situ* conditions point toward our measured rates being higher than *in situ* rates. Because every sample likely contains a mixture of different H_2 ases with different substrate specificities and exchange rates, it seems unlikely that activity will increase linearly with substrate concentration over several orders of magnitude. Still, it might be safe to assume that our measured rates overestimate *in situ* turnover by at least an order of magnitude, given the higher temperature, slurrying, and saturation with H_2 . With decreasing redox potential, H_2 plays an increasingly important role in electron-acceptor processes, so the level of overestimation may differ between redox zones. Nevertheless, the hydrogen oxidation rate measurements indicate potential for microbial activity regardless of the specific catabolic reaction (e.g., metal, SO_4^{2-} , or CO_2 reduction), and thus provide the opportunity to detect potential activity throughout the whole sediment column by a single method.

The ability to detect hydrogen oxidation and thus active microbial metabolism by using frozen samples is an advantage over methods that detect activity by measuring a metabolic rate, which requires metabolically active cells. Such methods usually require fresh, or rather non-frozen, sample material. Because the hydrogen oxidation measurement only targets

the intact H₂ase enzyme, microbial cells do not have to be kept alive until analysis. The only requirement is that the samples be frozen immediately after retrieval and kept under anoxic conditions. H₂ase-catalyzed hydrogen oxidation can thus be detected even after long periods of sample storage. This provides the opportunity to detect microbial activity in sediment retrieved during sampling campaigns where logistical or operational limitations do not allow immediate experimental treatment.

We used porewater chemical concentration profiles and the procedure of Wang et al. (2008) to calculate net turnover rates for relevant substrates at the individual sites. For each site, we separately calculated the turnover rate of the relevant metabolic compound (Figure 6). Perhaps unsurprisingly, we observe no significant correlation between potential volumetric hydrogen oxidation rates and calculated metabolic rates. There are several possible reasons for this lack of correlation. The calculated rates represent only net rates of production or consumption of single compounds, whereas our potential H₂ oxidation rate measurements provide a qualitative measure of the activity of the entire microbial community. As described by Wang et al. (2008) several metabolic activities can co-occur at the same depth, so any single calculation may fail to account for metabolic diversity. Although the porewater data from the Equatorial Pacific (EQP-05 and EQP-07) allowed calculation of turnover rates for several potentially co-existing metabolic processes, we found no correlation between the ensemble of metabolic rates and measured potential volumetric hydrogen oxidation rates. Due to this absence of correlation between calculated net turnover rates and measured H₂ oxidation rates, only qualitative assumptions about microbial activity can be made.

Although potential volumetric hydrogen oxidation rates cannot be translated directly into specific turnover rates, per-cell potential hydrogen oxidation rates can be compared within biogeochemical zones and across different zones.

Hydrogen Utilization Potential and Biogeochemical Zonation

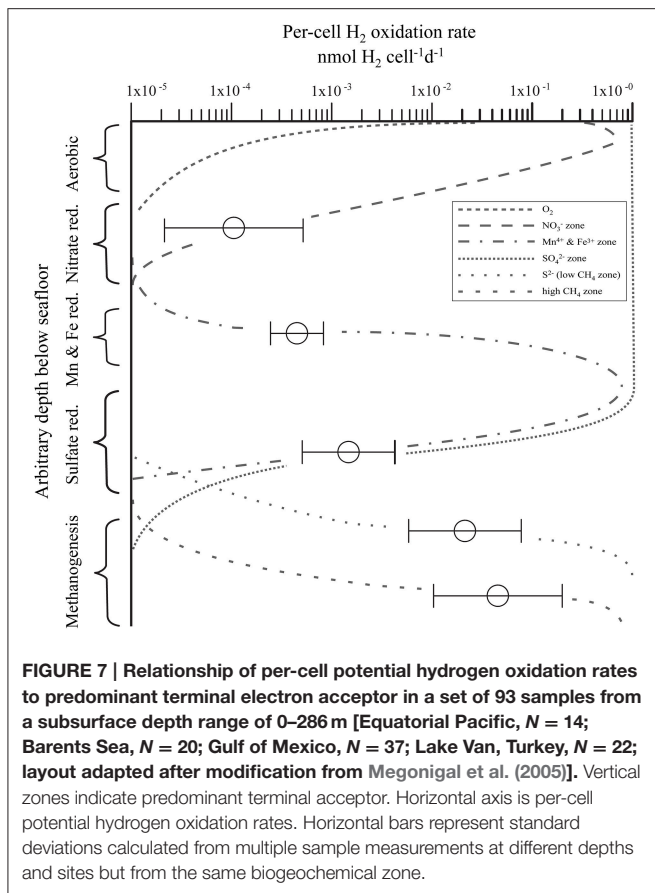
Because the volumetric potential hydrogen oxidation rate remains relatively constant with depth despite order-of-magnitude changes in cell abundance, we normalized potential hydrogen oxidation rate by dividing volumetric rates by the number of counted microbial cells (Figures 3–5). The counts include all cells that contain double-stranded DNA, irrespective of metabolic status or capability.

A recent study of Peters et al. (2015) estimated that only about 35% of all microorganisms encode for H₂ases, suggesting that H₂ases are not as ubiquitously distributed as previously thought (Soffientino et al., 2006). However, the findings of Peters et al. (2015) may not be fully applicable to subsurface environments as their study covered only 167 (5.7%) archaeal genomes. Archaea and bacteria have recently been reported to occur in roughly equal proportions in subseafloor sediment (Lloyd et al., 2013; Xie et al., 2013). Also, Fe-only H₂ases were not considered by Peters et al. (2015) but are found in many methanogenic archaea (Lyon

et al., 2004) that comprise a significant part of lacustrine and marine subsurface microbial communities (Lipp et al., 2008). In short, methanogenic and methanotrophic archaea are important players in subsurface ecosystems, and the data set of Peters et al. (2015) may not be representative of such environments. Rather, in the samples used in our study, the fraction of microbes that contain H₂ases is likely >35%. The fact that 93 (55%) of the 167 archaeal genomes covered by the study of Peters et al. (2015) contains [FeFe]- and [NiFe]-H₂ase homologs suggests that a higher percentage of archaea contain H₂ases. Even the most negative assumption, that only one third of all microbial cells contained H₂ases, would introduce a bias of a factor of three. This factor is dwarfed by the variation that we observe per-cell potential hydrogen oxidation rates, which range over four orders of magnitude from site to site (2×10^{-5} to 2×10^{-1} nmol H₂ cell⁻¹ d⁻¹; Figures 3–5). Given this variation in per-cell potential hydrogen oxidation rates, a potential factor-of-three bias in the assumed fraction of cells that encodes for H₂ases is insignificant.

We selected our sample set to the predominant electron-acceptor zones that typically occur in anoxic sediment (NO₃⁻ reduction, Mn⁴⁺ and Fe³⁺ reduction, SO₄²⁻ reduction, and methanogenesis zones). To identify common patterns in H₂ utilization, we grouped the samples into biogeochemical zones based on porewater composition. The first group contains all samples with detectable NO₃⁻ (NO₃⁻ zone). The second group contains samples where metal reduction predominates (Mn and Fe zone). The third group is defined by the presence of SO₄²⁻ and the absence of CH₄ (SO₄²⁻ zone). We subdivided samples with detectable CH₄ into a low-CH₄ (<0.6 μmol L⁻¹) zone and a high-CH₄ (>0.6 μmol L⁻¹) zone to separate samples with persistent but very low CH₄ even in the presence of dissolved SO₄²⁻ (e.g., IODP Exp. 308, BT Basin) from those with much higher CH₄ concentration and usually no SO₄²⁻. When plotting the per-cell potential hydrogen oxidation rate relative to the biogeochemical zones (Figure 7) the relationship between per-cell potential hydrogen oxidation activity and predominant metabolic process becomes obvious. Despite some scatter, per-cell potential hydrogen oxidation rates increase in the following order: NO₃⁻ zone < Mn⁴⁺ and Fe³⁺ zone < SO₄²⁻ zone < low CH₄ zone < high CH₄ zone. The lowest per-cell potential hydrogen oxidation rates (1.2×10^{-5} – 5×10^{-4} nmol H₂ cell⁻¹ d⁻¹) occur in the NO₃⁻ zone of site EQP-05 and site EQP-07. The metal reduction zone exhibits mean per-cell potential hydrogen oxidation rates that lie between those found in the NO₃⁻ and SO₄²⁻ reduction zones. Per-cell potential hydrogen oxidation rates in the SO₄²⁻ zone samples from Lake Van, Barents Sea, and the Equatorial Pacific mostly range between 5×10^{-4} and 4×10^{-3} nmol H₂ cell⁻¹ d⁻¹. In the low CH₄ zone (<0.6 μmol L⁻¹), they fall in the range of 5×10^{-3} to 8×10^{-2} nmol H₂ cell⁻¹ d⁻¹. In the high CH₄ zone (>0.6 μmol L⁻¹), rates are highest with values between 1×10^{-2} and 2×10^{-1} nmol H₂ cell⁻¹ d⁻¹.

There are multiple possible cause(s) of these differences in per-cell potential hydrogen oxidation rates between different redox (or predominant electron-acceptor) zones. They may be due to



differences in H₂ase enzyme kinetics or they may be related to *in situ* H₂ concentrations. Thus, in the less reducing zones, H₂ases need to be adapted to very low H₂ concentration resulting in lower k_m (Michaelis constant) values which often means lower V_{max} (maximum turnover rates), whereas in deeper layers, in which fermenters make up a higher proportion of the microbial community, H₂ concentration may be higher and the enzymes have a higher k_m and a higher V_{max} . As we carried out our incubations at uniformly high H₂ concentrations, H₂ases from deeper zones might be better adapted and work at a higher turnover rate.

With increasing sediment depth (or more precisely, age), organic matter becomes more recalcitrant. Although breakdown of macromolecular organic matter into biologically available monomers continues with increasing burial depth, the amount, and diversity of the bioavailable material decreases. Even highly complex organic molecules can be degraded by nitrate, metal, and sulfate reducers (Widdel and Rabus, 2001; Foght, 2008). In general, the substrate spectrum of microbes becomes smaller with decreasing redox potential, with methanogens having the smallest spectrum and reliant on fermenters to produce the narrow range of compounds (including H₂) that they can utilize. Thus, with increasingly reducing conditions, the fraction of organic matter that is fermented also increases, which is also concomitant to a greater production of H₂.

CONCLUSIONS

We measured potential hydrogen oxidation in all samples from multiple depths at several sites that collectively span a wide range of environmental conditions and biogeochemical zones. The ubiquity of this potential activity is consistent with ubiquity of H₂ utilization in subsurface marine and lacustrine sedimentary environments. Per-cell potential rates increases with increasing sediment depth, from one subsurface redox zone to another.

The tritium-based assay provides information about the microbial community's potential to utilize molecular H₂. It does not provide actual (*in situ*) rates, because the incubation conditions deviate in many ways from *in situ* conditions. Most obviously, the experimental setup forces all H₂ases to proceed in the net direction of splitting molecular H₂ to proton and electrons, irrespective of their role *in situ*. For example, H₂ases utilized by fermenters, which produce most of the H₂ in subsurface systems, also contribute to the measured H₂ oxidation rates, just like H₂ases that are used *in situ* for H₂ turnover by terminal oxidizers.

Nonetheless, this assay has potentially significant advantages. It can be used to detect potential microbial activity in subsurface sedimentary environments, regardless of predominant terminal electron-accepting process. And it can be applied to previously frozen sediment, which cannot usually be used for direct measurements of metabolic rates.

Per-cell potential hydrogen oxidation rates appear to vary with predominant electron acceptor at our sites. It is lowest in sediment where NO₃⁻ reduction predominates, and successively higher where metal (Mn⁴⁺ and Fe³⁺) reduction, SO₄²⁻ reduction, and CH₄ production (CO₂ reduction) predominates. Possible reasons for this relationship to predominant electron acceptor include (i) increasing importance of fermentation in successively deeper biogeochemical zones and (ii) adaptation of H₂ases to successively higher concentrations of H₂ in successively deeper zones.

AUTHOR CONTRIBUTIONS

RA and JK designed the study; RA, JK, JN, CG collected the samples; RA, JN, CA, AD, CG performed the laboratory work; RA, RM, AS, SD, CG, and JK interpreted data; RA wrote the paper; CG, SD, and JK edited the paper; all authors reviewed the manuscript.

ACKNOWLEDGMENTS

RA and JK were funded by the Federal Ministry of Education and Research (BMBF), Germany through the Forschungsverbundvorhaben GeoEn (Grant 03G0671A/B/C). JN was funded by LUNDIN Petroleum Norway. CG was funded by the German Science Foundation (DFG) through the ICDP Priority Program (SPP 1006) during the ICDP Expedition to Lake Van (KA2293/4-1) and currently by a Marie-Curie Individual Fellowship (grant agreement no. 327675). SD is funded by the NSF Division of Ocean Sciences (Grant 0939564). Portions of this material are based upon work supported

while RM was serving at the National Science Foundation. We thank the crews and scientific parties of the ICDP PaleoVan drilling campaign, R/V HU Sverdrup, R/V Knorr 195(III), and D/V JOIDES Resolution (Integrated Ocean Drilling Program Expedition 308). The R/V Knorr 195(III) expedition was

funded by the Biological Oceanography Program of the US National Science Foundation (Grant OCE-0752336). This is a contribution to the Deep Carbon Observatory (DCO). It is Center for Dark Energy Biosphere Investigations (C-DEBI) publication 317.

REFERENCES

- Adhikari, R. R., and Kallmeyer, J. (2010). Detection and quantification of microbial activity in the subsurface. *Chem. Erde-Geochem.* 70, 135–143. doi: 10.1016/j.chemer.2010.05.003
- Anderson, R. T., Chapelle, F. H., and Lovley, D. R. (2001). Comment on “Abiotic controls on H₂ production from basalt-water reactions and implications for aquifer biogeochemistry”. *Environ. Sci. Technol.* 35, 1553–1557. doi: 10.1021/es0015996
- Arnosti, C., Jørgensen, B. B., Sagemann, J., and Thamdrup, B. (1998). Temperature dependence of microbial degradation of organic matter in marine sediments: polysaccharide hydrolysis, oxygen consumption, and sulfate reduction. *Mar. Ecol. Prog. Ser.* 165, 59–70. doi: 10.3354/meps165059
- Bach, W., and Edwards, K. J. (2003). Iron and sulfide oxidation within the basaltic ocean crust: implications for chemolithoautotrophic microbial biomass production. *Geochim. Cosmochim. Acta* 67, 3871–3887. doi: 10.1016/S0016-7037(03)00304-1
- Bedard-Haughn, A., van Groenigen, J. W., and van Kessel, C. (2003). Tracing ¹⁵N through landscapes: potential uses and precautions. *J. Hydrol.* 272, 175–190. doi: 10.1016/S0022-1694(02)00263-9
- Blair, C. C., D’Hondt, S., Spivack, A. J., and Kingsley, R. H. (2007). Radiolytic hydrogen and microbial respiration in subsurface sediments. *Astrobiology* 7, 951–970. doi: 10.1089/ast.2007.0150
- Canfield, D. E., Jørgensen, B. B., Fossing, H., Glud, R., Gundersen, J., Ramsing, N. B., et al. (1993). Pathways of organic carbon oxidation in three continental margin sediments. *Mar. Geol.* 113, 27–40. doi: 10.1016/0025-3227(93)90147-N
- D’Hondt, S., Jørgensen, B. B., Miller, D. J., Batzke, A., Blake, R., Cragg, B. A., et al. (2004). Distributions of microbial activities in deep seafloor sediments. *Science* 306, 2216–2221. doi: 10.1126/science.1101155
- D’Hondt, S., Rutherford, S., and Spivack, A. J. (2002). Metabolic activity of subsurface life in deep-sea sediments. *Science* 295, 2067–2070. doi: 10.1126/science.1064878
- D’Hondt, S., Wang, G., and Spivack, A. J. (2014). “The underground economy (energetic constraints of seafloor life),” in *Earth and Life Processes Discovered from Seafloor Environments: A Decade of Science Achieved by the Integrated Ocean Drilling Program (IODP), Vol. 7*, eds R. Stein, D. K. Blackman, F. Inagaki, and H.-H. Larsen (Amsterdam: Elsevier), 127.
- Dixon, R. (1978). Nitrogenase - Hydrogenase interrelationships in Rhizobia. *Biochimie* 60, 233–236. doi: 10.1016/S0300-9084(78)80819-0
- Finke, N., and Jørgensen, B. B. (2008). Response of fermentation and sulfate reduction to experimental temperature changes in temperate and Arctic marine sediments. *ISME J.* 2, 815–829. doi: 10.1038/ismej.2008.20
- Flemings, P., Behrmann, J., John, C., and Scientists (2006). “Expedition reports Gulf of Mexico hydrogeology,” in *Proceedings of the IODP 308* (College Station, TX: IODP).
- Foght, J. (2008). Anaerobic biodegradation of aromatic hydrocarbons: pathways and prospects. *J. Mol. Microbiol. Biotechnol.* 15, 93–120. doi: 10.1159/000121324
- Fossing, H. (1995). “³⁵S-radiolabeling to probe biogeochemical cycling of sulfur,” in *Geochemical Transformations of Sedimentary Sulfur, Vol. 612*, eds M. A. Vairavamurthy and M. A. A. Schoonen (Washington, DC: American Chemical Society), 348–364.
- Froelich, P. N., Klinkhammer, G. P., Bender, M. L., Luedtke, N. A., Heath, G. R., Cullen, D., et al. (1979). Early oxidation of organic-matter in pelagic sediments of the eastern equatorial atlantic - suboxic diagenesis. *Geochim. Cosmochim. Acta* 43, 1075–1090. doi: 10.1016/0016-7037(79)90095-4
- Glombitza, C., Stockhecke, M., Schubert, C. J., Vetter, A., and Kallmeyer, J. (2013). Sulfate reduction controlled by organic matter availability in deep sediment cores from the saline, alkaline Lake Van (Eastern Anatolia, Turkey). *Front. Microbiol.* 4:209. doi: 10.3389/fmicb.2013.00209
- Häring, V., Klüber, H., and Conrad, R. (1994). Localization of atmospheric H₂-oxidizing soil hydrogenases in different particle fractions of soil. *Biol. Fertil. Soils* 18, 109–114. doi: 10.1007/BF00336455
- Hinrichs, K. U., Hayes, J. M., Bach, W., Spivack, A. J., Hmelo, L. R., Holm, N. G., et al. (2006). Biological formation of ethane and propane in the deep marine subsurface. *Proc. Natl. Acad. Sci. U.S.A.* 103, 14684–14689. doi: 10.1073/pnas.0606535103
- Hoehler, T. M., Albert, D. B., Alperin, M. J., Bebout, B. M., Martens, C. S., and Des Marais, D. J. (2002). Comparative ecology of H₂ cycling in sedimentary and phototrophic ecosystems. *Antonie van Leeuwenhoek* 81, 575–585. doi: 10.1023/A:1020517924466
- Hoehler, T. M., Alperin, M. J., Albert, D. B., and Martens, C. S. (1998). Thermodynamic control on hydrogen concentrations in an anoxic sediment. *Geochim. Cosmochim. Acta* 62, 1745–1756. doi: 10.1016/S0016-7037(98)0106-9
- Hoehler, T. M., Alperin, M. J., Albert, D. B., and Martens, C. S. (2001). Apparent minimum free energy requirements for methanogenic Archaea and sulfate-reducing bacteria in an anoxic marine sediment. *FEMS Microbiol. Ecol.* 38, 33–41. doi: 10.1111/j.1574-6941.2001.tb00879.x
- Holm, N. G., and Charlou, J. L. (2001). Initial indications of abiotic formation of hydrocarbons in the rainbow ultramafic hydrothermal system, Mid-Atlantic Ridge. *Earth Planet. Sci. Lett.* 191, 1–8. doi: 10.1016/S0012-821X(01)0397-1
- Holmkvist, L., Ferdelman, T. G., and Jørgensen, B. B. (2011). A cryptic sulfur cycle driven by iron in the methane zone of marine sediment (Aarhus Bay, Denmark). *Geochim. Cosmochim. Acta* 75, 3581–3599. doi: 10.1016/j.gca.2011.03.033
- Jørgensen, B. (1978a). A comparison of methods for the quantification of bacterial sulfate reduction in coastal marine sediments: II. Calculation from mathematical models. *Geomicrobiol. J.* 1, 29–47. doi: 10.1080/01490457809377722
- Jørgensen, B. B. (1978b). A comparison of methods for the quantification of bacterial sulfate reduction in coastal marine sediments 1. Measurement with radiotracer techniques. *Geomicrobiol. J.* 1, 11–27. doi: 10.1080/01490457809377721
- Jørgensen, B. B. (2000). “Bacteria and marine biogeochemistry,” in *Marine Geochemistry*, eds H. Schulz and M. Zabel (Berlin: Springer), 173–207.
- Jørgensen, B. B., Weber, A., and Zopfi, J. (2001). Sulfate reduction and anaerobic methane oxidation in Black Sea sediments. *Deep-Sea Res. Part I-Oceanogr. Res. Pap.* 48, 2097–2120. doi: 10.1016/S0967-0637(01)00007-3
- Kaden, H., Peeters, F., Lorke, A., Kipfer, R., Tomonaga, Y., and Karabiyikoglu, M. (2010). Impact of lake level change on deep-water renewal and oxic conditions in deep saline Lake Van, Turkey. *Water Resour. Res.* 46:W11508. doi: 10.1029/2009WR008555
- Kadioglu, M., Sen, Z., and Batur, E. (1997). The greatest soda-water lake in the world and how it is influenced by climatic change. *Ann. Geophys.* 15, 1489–1497. doi: 10.1007/s00585-997-1489-9
- Kallmeyer, J., Ferdelman, T. G., Weber, A., Fossing, H., and Jørgensen, B. B. (2004). A cold chromium distillation procedure for radiolabeled sulfide applied to sulfate reduction measurements. *Limnol. Oceanogr. Methods* 2, 171–180. doi: 10.4319/lom.2004.2.171

- Kallmeyer, J., Grewe, S., Glombitza, C., and Kitte, J. A. (2015). Microbial abundance in lacustrine sediments: a case study from Lake Van, Turkey. *Int. J. Earth Sci.* 104, 1667–1677. doi: 10.1007/s00531-015-1219-6
- Kallmeyer, J., Pockalny, R., Adhikari, R. R., Smith, D. C., and D'Hondt, S. (2012). Global distribution of microbial abundance and biomass in seafloor sediment. *Proc. Natl. Acad. Sci. U.S.A.* 109, 16213–16216. doi: 10.1073/pnas.1203849109
- Kallmeyer, J., Smith, D. C., Spivack, A. J., and D'Hondt, S. (2008). New cell extraction procedure applied to deep subsurface sediments. *Limnol. Oceanogr. Methods* 6, 236–245. doi: 10.4319/lom.2008.6.236
- Kempe, S., Kazmierczak, J., Landmann, G., Konuk, T., Reimer, A., and Lipp, A. (1991). Largest known microbialites discovered in Lake Van, Turkey. *Nature* 349, 605–608. doi: 10.1038/349605a0
- Laanbroek, H. J., and Veldkamp, H. (1982). Microbial interactions in sediment communities. *Philos. Trans. R. Soc. Lond. B. Biol. Sci.* 297, 533–550. doi: 10.1098/rstb.1982.0059
- Lin, L.-H., Slater, G. F., Sherwood Lollar, B., Lacrampe-Couloume, G., and Onstott, T. C. (2005). The yield and isotopic composition of radiolytic H₂, a potential energy source for the deep subsurface biosphere. *Geochim. Cosmochim. Acta* 69, 893–903. doi: 10.1016/j.gca.2004.07.032
- Lipp, J. S., Morono, Y., Inagaki, F., and Hinrichs, K.-U. (2008). Significant contribution of Archaea to extant biomass in marine subsurface sediments. *Nature* 454, 991–994. doi: 10.1038/nature07174
- Litt, T., Anselmetti, F. S., Baumgarten, H., Beer, J., Cagatay, N., Cukur, D., et al. (2012). 500,000 Years of environmental history in eastern Anatolia: the PALEOVAN drilling project. *Sci. Drill.* 14, 18–29. doi: 10.5194/sd-14-18-2012
- Litt, T., Krastel, S., Sturm, M., Kipfer, R., Orcen, S., Heumann, G., et al. (2009). 'PALEOVAN', International Continental Scientific Drilling Program (ICDP): site survey results and perspectives. *Quat. Sci. Rev.* 28, 1555–1567. doi: 10.1016/j.quascirev.2009.03.002
- Lloyd, K. G., May, M. K., Kevorkian, R. T., and Steen, A. D. (2013). Meta-analysis of quantification methods shows that archaea and bacteria have similar abundances in the seafloor. *Appl. Environ. Microbiol.* 79, 7790–7799. doi: 10.1128/AEM.02090-13
- Long, H., Flemings, P., Germaine, J., Saffer, D., and Dugan, B. (2008). "Data report: consolidation characteristics of sediments from IODP Expedition 308, Ursa Basin, Gulf of Mexico", in *Proceedings of the IODP, 308*, eds P. B. Flemings, J. H. Behrmann, C. M. John, and the Expedition 308 Scientists (College Station, TX: Integrated Ocean Drilling Program Management International Inc.).
- Lyon, E. J., Shima, S., Buurman, G., Chowdhuri, S., Batschauer, A., Steinbach, K., et al. (2004). UV–A/blue–light inactivation of the 'metal–free' hydrogenase (Hmd) from methanogenic archaea. *Eur. J. Biochem.* 271, 195–204. doi: 10.1046/j.1432-1033.2003.03920.x
- Manheim, F. T. (1966). A hydraulic squeezer for obtaining interstitial water from consolidated and unconsolidated sediments. *USGS Ref. Pap.* 550, 171–174.
- Martens, C. S., and Berner, R. A. (1974). Methane production in the interstitial waters of sulfate-depleted marine sediments. *Science* 185, 1167–1169. doi: 10.1126/science.185.4157.1167
- Megonigal, J. P., Hines, M. E., and Visscher, P. T. (2005). "Anaerobic metabolism: linkages to trace gases and aerobic processes," in *Treatise on Geochemistry*, eds H. D. Holland and K. K. Turekian (Oxford: Pergamon), 317–424.
- Middelburg, J. J. (1989). A simple rate model for organic-matter decomposition in marine-sediments. *Geochim. Cosmochim. Acta* 53, 1577–1581. doi: 10.1016/0016-7037(89)90239-1
- Mitterer, R. M., Malone, M. J., Goodfriend, G. A., Swart, P. K., Wortmann, U. G., Logan, G. A., et al. (2001). Co-generation of hydrogen sulfide and methane in marine carbonate sediments. *Geophys. Res. Lett.* 28, 3931–3934. doi: 10.1029/2001GL013320
- Morono, Y., Terada, T., Masui, N., and Inagaki, F. (2009). Discriminative detection and enumeration of microbial life in marine subsurface sediments. *ISME J.* 3, 503–511. doi: 10.1038/ismej.2009.1
- Nealson, K. H. (2005). Hydrogen and energy flow as "sensed" by molecular genetics. *Proc. Natl. Acad. Sci. U.S.A.* 102, 3889–3890. doi: 10.1073/pnas.0500211102
- Nealson, K. H., Inagaki, F., and Takai, K. (2005). Hydrogen-driven subsurface lithoautotrophic microbial ecosystems (SLiMEs): do they exist and why should we care? *Trends Microbiol.* 13, 405–410. doi: 10.1016/j.tim.2005.07.010
- Nickel, J. C., Di Primio, R., Mangelsdorf, K., Stoddart, D., and Kallmeyer, J. (2012). Characterization of microbial activity in pockmark fields of the SW-Barents Sea. *Mar. Geol.* 332, 152–162. doi: 10.1016/j.margeo.2012.02.002
- Nunoura, T., Soffientino, B., Blazejak, A., Kakuta, J., Oida, H., Schippers, A., et al. (2009). Seafloor microbial communities associated with rapid turbidite deposition in the Gulf of Mexico continental slope (IODP Expedition 308). *FEMS Microbiol. Ecol.* 69, 410–424. doi: 10.1111/j.1574-6941.2009.00718.x
- Odom, J. M., and Peck, H. D. Jr. (1984). Hydrogenase, electron-transfer proteins, and energy coupling in the sulfate-reducing bacteria *Desulfovibrio*. *Annu. Rev. Microbiol.* 38, 551–592. doi: 10.1146/annurev.mi.38.100184.003003
- Peters, J. W., Schut, G. J., Boyd, E. S., Mulder, D. W., Shepard, E. M., Broderick, J. B., et al. (2015). [FeFe]- and [NiFe]-hydrogenase diversity, mechanism, and maturation. *Biochim. Biophys. Acta* 1853, 1350–1369. doi: 10.1016/j.bbamcr.2014.11.021
- Reimer, A., Landmann, G., and Kempe, S. (2009). Lake Van, eastern anatolia, hydrochemistry and history. *Aquat. Geochem.* 15, 195–222. doi: 10.1007/s10498-008-9049-9
- Røy, H., Kallmeyer, J., Adhikari, R. R., Pockalny, R., Jørgensen, B. B., and D'Hondt, S. (2012). Aerobic microbial respiration in 86-million-year-old deep-sea red clay. *Science* 336, 922–925. doi: 10.1126/science.1219424
- Sagemann, J., Jørgensen, B. B., and Greeff, O. (1998). Temperature dependence and rates of sulfate reduction in cold sediments of Svalbard, Arctic Ocean. *Geomicrobiol. J.* 15, 85–100. doi: 10.1080/01490459809378067
- Sauer, P., Glombitza, C., and Kallmeyer, J. (2012). A system for incubations at high gas partial pressure. *Front. Microbiol.* 3:25. doi: 10.3389/fmicb.2012.00025
- Schink, B., Lupton, F. S., and Zeikus, J. G. (1983). Radioassay for hydrogenase activity in viable cells and documentation of aerobic hydrogen-consuming bacteria living in extreme environments. *Appl. Environ. Microbiol.* 45, 1491–1500.
- Schrump, H. N., Murray, R. W., and Gribsholt, B. (2012). Comparison of Rhizon sampling and whole round squeezing for marine sediment porewater. *Sci. Drill.* 13, 47–50. doi: 10.5194/sd-13-47-2012
- Seeberg-Elverfeldt, J., Schlüter, M., Feseker, T., and Kölling, M. (2005). Rhizon sampling of porewaters near the sediment–water interface of aquatic systems. *Limnol. Oceanogr. Methods* 3, 361–371. doi: 10.4319/lom.2005.3.361
- Soffientino, B., Spivack, A. J., Smith, D. C., and D'Hondt, S. (2009). Hydrogenase activity in deeply buried sediments of the Arctic and North Atlantic Oceans. *Geomicrobiol. J.* 26, 537–545. doi: 10.1080/01490450903104232
- Soffientino, B., Spivack, A. J., Smith, D. C., Roggenstein, E. B., and D'Hondt, S. (2006). A versatile and sensitive tritium-based radioassay for measuring hydrogenase activity in aquatic sediments. *J. Microbiol. Methods* 66, 136–146. doi: 10.1016/j.mimet.2005.11.004
- Solheim, A. (1991). *The Depositional Environment of Surging Sub-polar Tidewater Glaciers: A Case Study of the Morphology, Sedimentation and Sediment Properties in a Surge Affected Marine Basin Outside Nordaustlandet, Northern Barents Sea, Vol. 197*. Norsk Polarinstittut. Skrifter.
- Spear, J. R., Walker, J. J., McCollom, T. M., and Pace, N. R. (2005). Hydrogen and bioenergetics in the Yellowstone geothermal ecosystem. *Proc. Natl. Acad. Sci. U.S.A.* 102, 2555–2560. doi: 10.1073/pnas.0409574102
- Stevens, T. O., and McKinley, J. P. (1995). Lithoautotrophic microbial ecosystems in deep basalt aquifers. *Science* 270, 450–454. doi: 10.1126/science.270.5235.450
- Teske, A. P. (2012). Tracking microbial habitats in seafloor sediments. *Proc. Natl. Acad. Sci. U.S.A.* 109, 16756–16757. doi: 10.1073/pnas.1215867109
- Thamdrup, B., and Fleischer, S. (1998). Temperature dependence of oxygen respiration, nitrogen mineralization, and nitrification in arctic sediments. *Aquat. Microb. Ecol.* 15, 191–199. doi: 10.3354/ame015191
- Treude, T., Boetius, A., Knittel, K., Wallmann, K., and Jørgensen, B. B. (2003). Anaerobic oxidation of methane above gas hydrates at Hydrate Ridge, NE Pacific Ocean. *Mar. Ecol. Prog. Ser.* 264, 1–14. doi: 10.3354/meps264001
- Treude, T., Niggemann, J., Kallmeyer, J., Wintersteller, P., Schubert, C. J., Boetius, A., et al. (2005). Anaerobic oxidation of methane and sulfate reduction along the Chilean continental margin. *Geochim. Cosmochim. Acta* 69, 2767–2779. doi: 10.1016/j.gca.2005.01.002

- Vignais, P. M., and Billoud, B. (2007). Occurrence, classification, and biological function of hydrogenases: an overview. *Chem. Rev.* 107, 4206–4272. doi: 10.1021/cr050196r
- Vuillemin, A., Ariztegui, D., and Team, P. S. (2013). Geomicrobiological investigations in subsaline maar lake sediments over the last 1500 years. *Quat. Sci. Rev.* 71, 119–130. doi: 10.1016/j.quascirev.2012.04.011
- Wang, G. Z., Spivack, A. J., Rutherford, S., Manor, U., and D'Hondt, S. (2008). Quantification of co-occurring reaction rates in deep seafloor sediments. *Geochim. Cosmochim. Acta* 72, 3479–3488. doi: 10.1016/j.gca.2008.04.024
- Widdel, F., and Rabus, R. (2001). Anaerobic biodegradation of saturated and aromatic hydrocarbons. *Curr. Opin. Biotechnol.* 12, 259–276. doi: 10.1016/S0958-1669(00)00209-3
- Xie, S., Lipp, J. S., Wegener, G., Ferdelman, T. G., and Hinrichs, K.-U. (2013). Turnover of microbial lipids in the deep biosphere and growth of benthic archaeal populations. *Proc. Natl. Acad. Sci. U.S.A.* 110, 6010–6014. doi: 10.1073/pnas.1218569110
- Zeikus, J. G. (1977). The biology of methanogenic bacteria. *Bacteriol. Rev.* 41, 514–541.
- Zhabina, N. N., and Volkov, I. I. (1978). “A method of determination of various sulfur compounds in sea sediments and rocks,” in *Environmental Biogeochemistry and Geomicrobiology*, ed W. E. Krumbein (Ann Arbor, MI: Ann Arbor Science), 735–745.

Conflict of Interest Statement: The authors declare that the research was conducted in the absence of any commercial or financial relationships that could be construed as a potential conflict of interest.

Copyright © 2016 Adhikari, Glombitza, Nickel, Anderson, Dunlea, Spivack, Murray, D'Hondt and Kallmeyer. This is an open-access article distributed under the terms of the Creative Commons Attribution License (CC BY). The use, distribution or reproduction in other forums is permitted, provided the original author(s) or licensor are credited and that the original publication in this journal is cited, in accordance with accepted academic practice. No use, distribution or reproduction is permitted which does not comply with these terms.